ACS OMEGA

Open Access

http://pubs.acs.org/journal/acsodf

Article

Drug Polymeric Carrier of Aceclofenac Based on Amphiphilic Chitosan Micelles

Noof A. Alenazi,* Mohammed G. Bokhari, Mohammed A.S. Abourehab, and Mostafa R. Abukhadra

Cite This: *ACS Omega* 2023, 8, 48145−48158

Read Online

ACCESS | Metrics & More | Article Recommendations | Supporting Information

ABSTRACT: Amphiphilic micelles based on chitosan (CS) were applied as drug carriers of aceclofenac (ACF) as a potential method to induce its bioavailability and therapeutic efficiency. *N*-octyl-*N*,*O*-succinyl CS (OSCS), an amphiphilic CS derivative, was successfully synthesized and loaded physically by ACF at different pH values and using different dosages of ACF, forming ACF-loaded polymeric micelles (PMs). The obtained PMs and ACF-loaded PMs were characterized by different analytical techniques, including AFM, TEM, DLS, UV−vis spectrophotometry, ^{1}H NMR spectroscopy, and FT-IR spectroscopy. The pH 5 sample with a 30% ACF/polymer ratio showed the highest ACF loading capacity (LC) and entrapment efficiency (EE). In vitro release behaviors of pure ACF and ACF-loaded PMs at each release point indicated that the release profile of pH-responsive PMs loaded with ACF demonstrated quicker release rates (94% after 480 min) compared to the release behavior noticed for free ACF (59.56% after 480 min). Furthermore, the release rates exhibit a notable rise when the pH is increased from 1.2 to 4.7. In the carrageenan-induced inflammation model of paw edema in rats, it has been demonstrated that the injection of ACF-loaded PMs (at a dose of 10 mg/kg) resulted in a strengthened inflammatory activity compared to the injection of free ACF at equivalent dosages as well as at time intervals. However, the use of ACF-loaded PMs for a duration of 6 h displayed a notable reduction of paw edema, with an inhibition percentage of 85.09%, in contrast to the 74.9% inhibition percentage observed for the free ACF medication.

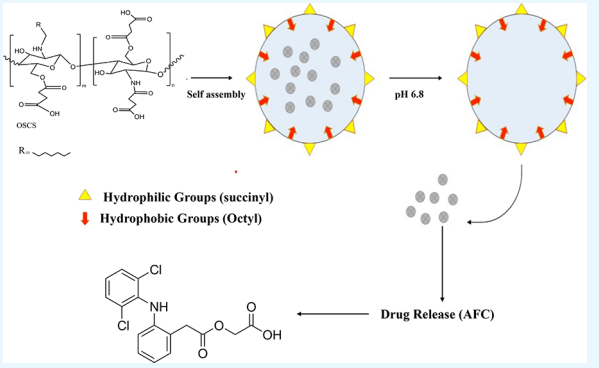

1. INTRODUCTION

CS is a unique polysaccharide biopolymer produced from chitin by alkaline deacetylation from crustacean sources. Although it may also be found naturally in Mucoraceae fungus cell walls,[1] CS includes both primary and secondary free hydroxyl groups, as well as a primary amino group.[2] The presence of amino groups distinguishes CS from chitin, which impacts its solubility in dilute acids. CS is the only positively charged polysaccharide found in nature with protonated amino groups that can form ionic complexes with a wide spectrum of natural or synthetic anionic species, including lipids, proteins, DNA, and specific negatively charged synthetic polymers.[3] CS's polymeric chain is described as a copolymer structure containing D-glucosamine and *N*-acetyl residues. Most of the *N*-acetyl groups are hydrolyzed.[4]

CS is nontoxic, biodegradable, and biocompatible, and it has been authorized for wound dressings and nutritional use by the Food and Drug Administration (FDA). It has the probability of altering drug surface characteristics, the duration of sustained release, and the distribution of target nanoparticles in organs or cells. These appealing properties give CS considerable attention in agriculture, the food industry, biotechnology, pharmacy, and biomedicine to develop hemodialysis membranes, artificial skin, drug targeting, and the development of conventional and novel medication delivery methods.[5] Many drugs have low bioavailability in the oral route due to low hydrophilic properties, fast degradation in a highly acidic environment (stomach pH), or slow absorption from the gastrointestinal tract. Therefore, a CS-based delivery device with good hydrophilic properties could be the answer to enhancing the bioavailability of oral medications because of its numerous advantages.[6]

CS possesses a positive charge as it is a naturally cationic biopolymer in its dissolved form (pH < 5,7) and has chelating, antimicrobial, gelling, and film-forming properties, which give it a capability for multiple uses.[7,8] CS antibacterial characteristics can be explained in a variety of ways. The most accepted theory holds that CS interferes with the negatively charged cell membrane, rupturing it and altering its permeability. As a result, components leak out of the bacterial cells, causing cell

Received: September 15, 2023
Revised: November 17, 2023
Accepted: November 24, 2023
Published: December 5, 2023

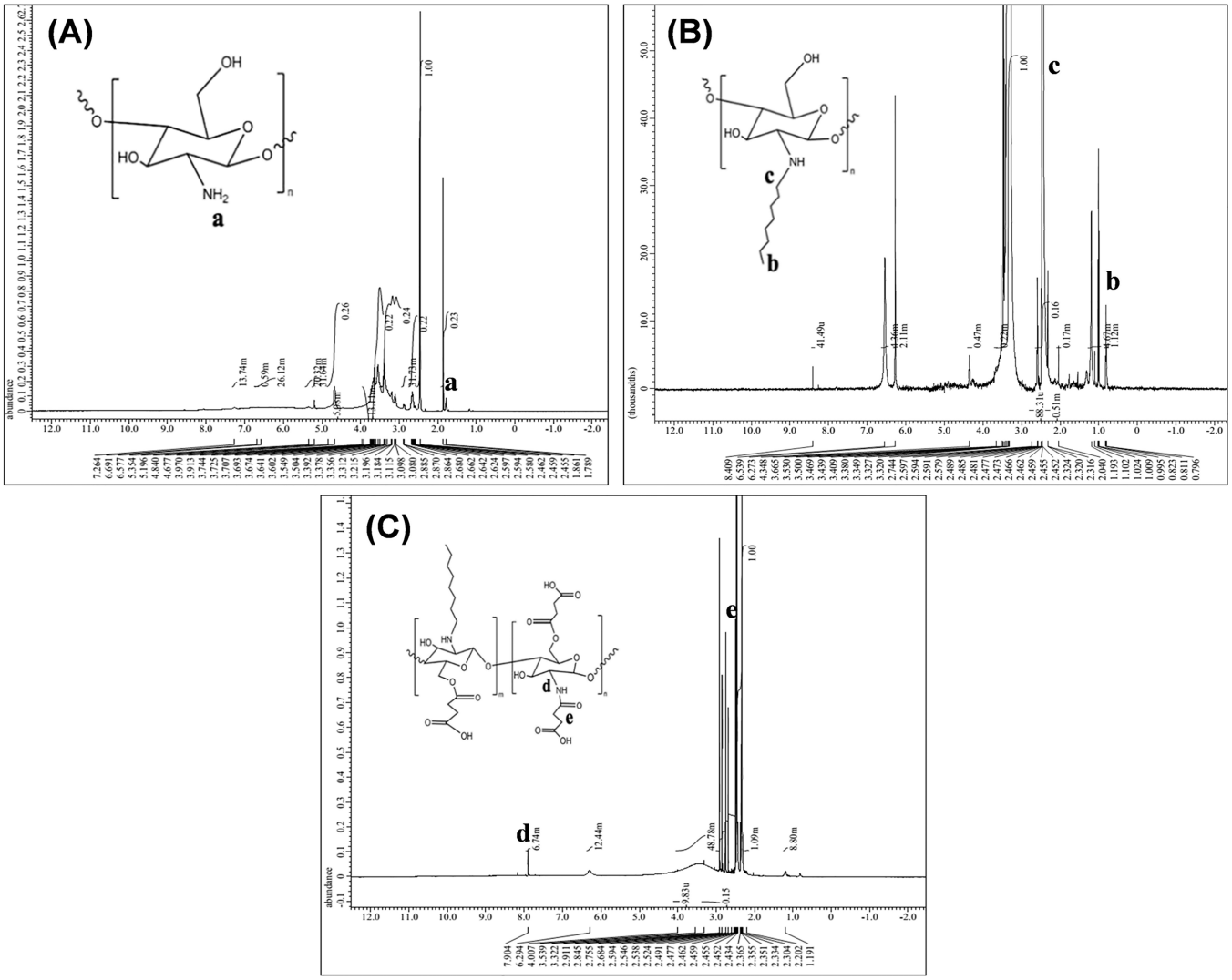

Figure 1. ^{1}H NMR spectra of CS (A), OCS (B), and OSCS (C).

death. Because of its limited solubility above pH 6.5, CS exhibits antibacterial action only in an acidic environment.[9−11] CS's antibacterial action is influenced by several variables, including the chitin type, degree of polymerization, molecular weight, solvent, specific physicochemical characteristics, and the solution's pH. In some studies, it was found that because of the difference in cell walls between Gram (−) and Gram (+) bacteria, CS's antibacterial action is greater against Gram (+) bacteria than against Gram (−) bacteria. In other studies, gram-negative bactericidal effects have been observed to be more significant compared to Gram-positive bacteria.[9,12]

CS polymeric micelles have been the subject of numerous studies using various techniques and preparations, such as quaternized CS, *N*-acylated CS, or cross-linked CS, to reduce the toxicity or improve the absorption of various drugs.[13−15] They have also been used as drug carriers to improve the delivery of oral, nasal, mucosal, gene, buccal, and vaccine medications.[15] In this study, we decided to encapsulate NSAID ACF inside chitosan nanoparticles to overcome its drawbacks. There have been past studies on NSAIDs like ibuprofen, naproxen, and Meloxicam, but none on ACF has been studied.[16−18]

Oral ACF is a phenylacetic acid derivative of NSAIDS that affects a number of inflammatory mediators. ACF is an analgesic and anti-inflammatory drug that offers pain relief for a wide range of medical diseases and symptoms. The medicine lowers pain, reduces disease severity, and improves the knee's functional capability in individuals with knee osteoarthritis. ACF reduces joint inflammation, pain intensity, and the duration of morning stiffness in patients with rheumatoid arthritis. It is also beneficial for various painful disorders, such as dental or gynecological conditions. ACF has been demonstrated to influence a wide range of inflammation-related mediators. ACF inhibits cytokines interleukin-1 (IL-1) and tumor necrosis factor (TNF) synthesis, as well as prostaglandin E2 (PGE2) production. Effects on cell adhesion molecules from neutrophils have also been noted. The inhibitory effects of ACF on synovial levels of PGE2 have been confirmed in patients with acute knee pain and synovial fluid effusions. In vitro data indicate the inhibition of COX-1 and -2 by ACF in whole blood assays, with the selectivity for COX-2 being evident. As soon as it is taken orally, ACF quickly enters the bloodstream and reaches peak plasma concentrations (Cmax) within 1.25 to 3 h. The volume of distribution (Vd) is approximately 25 L, and the drug is highly protein-bound (>99%) in plasma. ACF's suggested dose is 100 mg twice daily. Patients with hepatic impairment should have their dose reduced to 100 mg once daily. Those with renal,

https://doi.org/10.1021/acsomega.3c07065
ACS Omega 2023, 8, 48145−48158

hepatic, or cardiovascular impairment and those taking other medications should be cautious when using ACF, especially the elderly.[19]

Although there are numerous benefits to using ACF, there are also some drawbacks, such as gastrointestinal bleeding and ulcers. Patients prefer oral medication administration because it is convenient, provides the greatest control over overdose schedules, and is less likely to cause problems during administration. Oral drug administration is the most prevalent and preferred method of drug delivery, even though it also has some key drawbacks, such as the first-pass effect and digestive enzyme breakdown as well as a late onset of action. Amphiphilic micelles might be a good solution for overcoming ACF side effects and oral route drawbacks. Polymeric drug micelles can therefore be used to increase the bioavailability and efficacy of ACF and minimize its side effects by creating a prolonged release of the medication.[20,21] Polymerized medicine drug delivery via micelles has become a common practice in recent years, in which the micelle hydrophobic core holds hydrophobic drugs and the hydrophilic shell keeps a balance between them and their surrounding water environments, ensuring minimal systemic toxicities and enhancing the treatment efficacy.[22−24]

Since ACF is hydrophobic, altering the CS backbone with hydrophobic groups like octyl groups might improve the interaction between ACF and the inner core of CS PMs, thereby boosting ACF LC. Thus, the goal of this research project is to produce an amphiphilic micelle that is CS-based and contains ACF in order to boost its bioavailability and extend its medication release while avoiding its negative effects on the gastrointestinal tissues. Amphiphilic micelles are generated by the self-assembly of hydrophilic and hydrophobic unimers in solution. The self-assembly of water-insoluble (hydrophobic) medicines occurs in aqueous solutions. In this work, the hydrophobic core of the micelle retains hydrophobic medications, while the hydrophilic shell maintains a balance between them and the aqueous surroundings around them, guaranteeing minimum systemic toxicity and boosting the therapeutic efficacy (Figure 1A).

2. RESULTS AND DISCUSSION

The amphiphilic OSCS has been synthesized following a procedure done by Woraphatphadung et al.[25] The OSC derivative has been prepared by a two-step process in which the hydrophobic group was first introduced using octanal Schiff base intermediates[25] following a reduction reaction by $NaBH_4$.[26] Then, the hydrophilic groups were attached to the polymer backbone using succinic anhydride in a mixture of solvents (DMF and DMSO) at 100 °C under a nitrogen atmosphere through an opening ring reaction in which the succinic molecules were linked to both *N* and *O* sites in the CS backbone.[27]

2.1. Amphiphilic OSCS Characterization. CS, OCS, OSCS, and ACF-loaded PMs were characterized using ^{1}HNMR and FT-IR to confirm their structures and the successful preparation. The ^{1}H NMR spectra of CS, OCCS, and OSCS are provided. The CS spectrum (Figure 1A) showed a rough $-NH_2$ proton signal (**a**) at 1.7 ppm,[28] while the OCS spectrum (Figure 1B) exhibited similar signals as the pure CS except for two additional proton signals at 0.8 and 2.5 ppm because of the presence of the methyl (**b**) and methylene (**c**) moieties for the hydrocarbon chain. On the other hand, the OSCS spectrum (Figure 1C) showed the exact proton signals of the OCS besides the additional proton signal at 2.6 ppm (**e**) because of the presence of the methylene protons of the succinyl groups. The −NH proton of OSCS (**d**) was also noticed to be deshielded to 7.9 ppm due to the C═O amide stretching band.[29]

FT-IR analysis was used to check the quality of our OSCS PMs and to see whether they were properly produced. The FT-IR spectra of CS, OCS, and OSCS are shown in Figure 2.

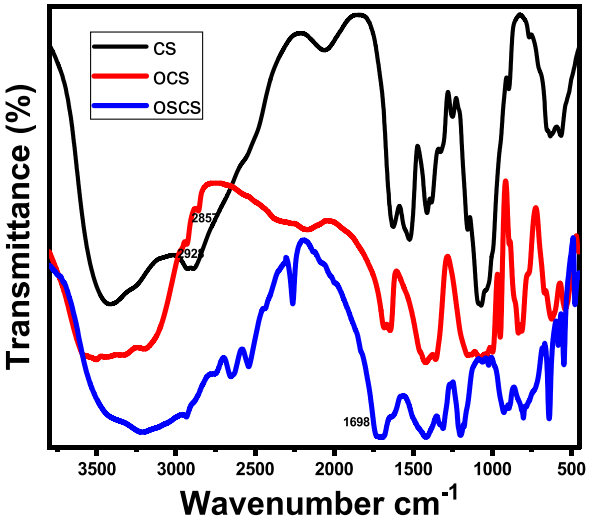

Figure 2. FT-IR spectra of CS, OCS, and OSCS.

As seen, the OCS spectrum exhibited peaks similar to that of pure CS except for the presence of the alkyl C−H stretching absorption peaks that are shown at both 2928 and 2857 cm^{-1}, which are assigned to the octyl moiety, and N−C.[30] On the other hand, the OSCS spectrum showed a distinct absorption peak at 1689 cm^{-1} assigned to the presence of a C═O amide stretching band due to the attachment of succinic groups, in which our data came in agreement with previously reported works.[26,31] Therefore, ^{1}H NMR and FT-IR analyses indicate the successful preparation of OCS and OSCS by the *N*-amination reaction, followed by an *N*,*O*-succinylation reaction.

2.2. TEM, DLS, and AFM Analyses. The morphologies and particle sizes of the PMs before and after the addition of ACF were examined using TEM, DLS, and AFM in order to have a better understanding of the release behavior of ACF from OSCS PMs as a function of pH. Due to drug encapsulation, the diameters of ACF-loaded PMs (11.7−13.5 nm) were greater than those of blank PMs (6.5−7.5 nm), according to DLS data (Figure 3). As previous studies have shown,[32,33] our PMs got bigger in size after being encapsulated with ACF, which indicates the success of ACF trapping inside the micelles. As the weight ratio of ACF to polymer increases, the average PM size tends to rise. Self-aggregation may occur because of the larger particle size of the ACF-loaded PMs. In TEM and AFM pictures, the self-assembled PMs showed self-aggregates with a regular spherical shape.[34] However, the size of the PMs only altered when various pH media were applied.[35] The strongly protonated carboxyl groups of succinic acid caused the PMs to cluster into microparticles at pH 1.2.[36] The AFM study confirmed that the morphologies and particle sizes of PMs before and after ACF was loaded changed when the pH varied due to the ionizable succinic acid groups on the PM surface. The PMs had a spherical morphology with

https://doi.org/10.1021/acsomega.3c07065
ACS Omega 2023, 8, 48145−48158

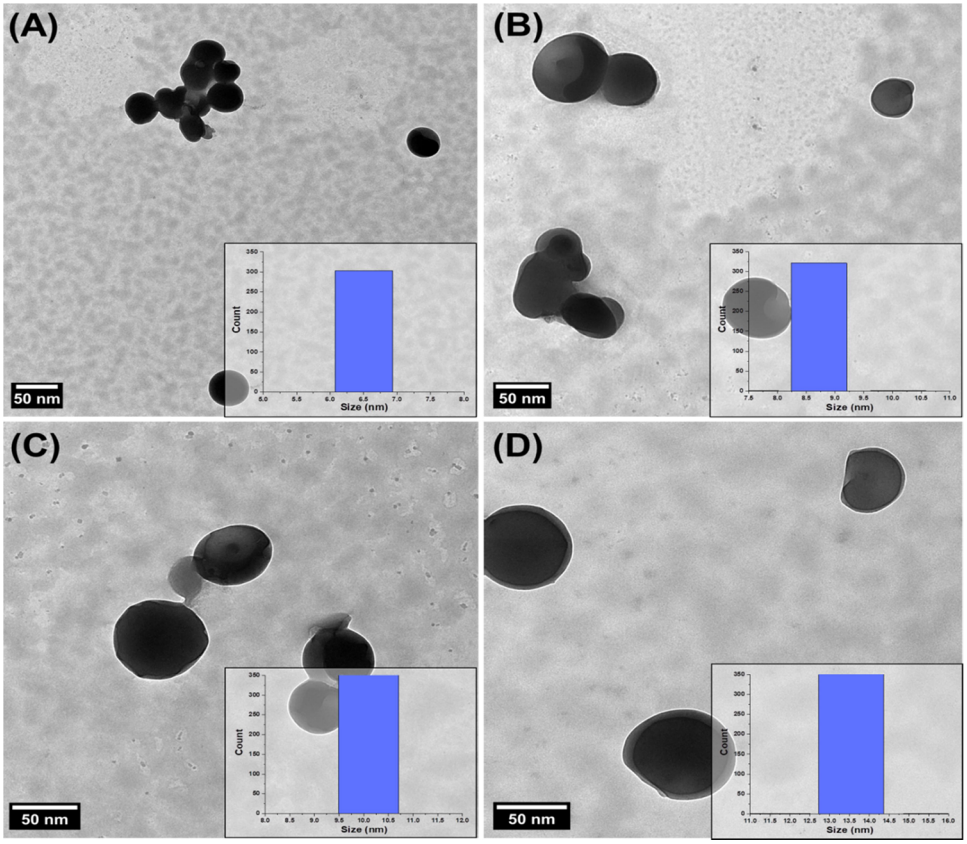

Figure 3. DLS and TEM results of (a) OSCS, (b) OSCS with 10% ACF, (c) OSCS with 20% ACF, and (d) OSCS with 30% ACF.

aggregation, implying substantial swelling to promote the release of ACF from the PMs (Figure 4).[37,38]

2.3. XRD Analysis. The CS diffractogram (Figure S1) showed an amorphous structure by showing several small diffraction peaks in the range of 2θ = 10°−20° and 2θ = 20°−30°, which comes in agreement with previous studies,[39,40] whereas the crystal structure of ACF particles in Figure S2 showed diffraction peaks at 2θ = 16.5°, 21.8°, 23.9°, 25.2°, 25.6°, and 31°, which came in agreement with the reported data.[41] The presence of ACF in PMs was confirmed using the XRD patterns (Figure 5). There were several peaks at 2θ = 16.5°, 21.8°, 23.9°, 25.2°, 25.6°, and 31° in the XRD diagram of ACF, as well as a significant number of tiny peaks in the region of 30°−55°. For some reason, the potency of ACF was reduced when it was physically mixed with PMs. However, the physical mixing of ACF and PMs still exhibited a reduced intensity of ACF's usual peak. There was also a minor ACF peak in ACF-loaded PMs, which had a spectrum similar to that of the blank micelles, although the ACF peak was unnoticeable. This means that ACF was completely trapped in the OSCS PMs at the molecular level, which might improve medication absorption.[41,42]

2.4. Thermal Analysis. DSC and TGA were used to determine the heat stabilities of ACF, CS, OCS, OSCS, and ACF-loaded PMs. The TGA thermograms of CS, OCS, and OSCS were investigated, as shown in Figure 6. The thermal decomposition of CS was similar to OSCS decomposition in which they both exhibited two weight losses: the first loss at 100 °C (15%) due to the presence of moisture from the two polymers; and the second major loss at 250 °C (55% for CS and 70% for OSCS) due to the polysaccharide polymer degradation[25] and succinic acid moieties in OSCS.[25,42] On the OCS was shown two different weight losses at 100 °C (23%), and the second loss at 300 °C (50%) corresponds to the moisture vaporization and the high-molecular-weight polymer decomposition because of the presence of octyl groups (hydrophobic portion). It can be clearly seen that the presence of hydrophobic and hydrophilic moieties caused an alternation in CS thermal stability.[31]

DSC was also used to examine the impact of chemical alteration on ACF, CS, OSCS, and ACF-loaded PMs with thermal disintegration. DSC analysis was used to assess the physical state of ACF in the PMs. The melting endothermic event is seen in Figure 7A, with an onset at 152.74 °C and an end set at 166.7 °C in the DSC spectrum of pure ACF powder at 159.65 °C. According to its DSC spectrum in Figure 7B, CS has a broad endothermic peak of about 100 °C and an exothermic peak of 340 °C. The removal of moisture and other probable volatile losses from the CS matrix might account for the occurrence of the endothermic peak. The degradation of the saccharide structure in CS may be responsible for the exothermic peak. The OSCS DSC spectrum (Figure 7C) indicates the endothermic melting peak changes at lower temperatures of roughly 50−60 °C, clearly demonstrating the influence of CS substitution with octyl and succinyl groups on the degree of polymer crystallinity. According to these findings, the addition of substitution groups to CS molecules reduced their thermal stability while increasing their water solubility.[43,44]

The spectrum of the ACF-loaded PMs, on the other hand, revealed two endothermic peaks: the first was around 150−160 °C for both pH 6−8 and pH 5 samples, in line with the

https://doi.org/10.1021/acsomega.3c07065
ACS Omega 2023, 8, 48145−48158

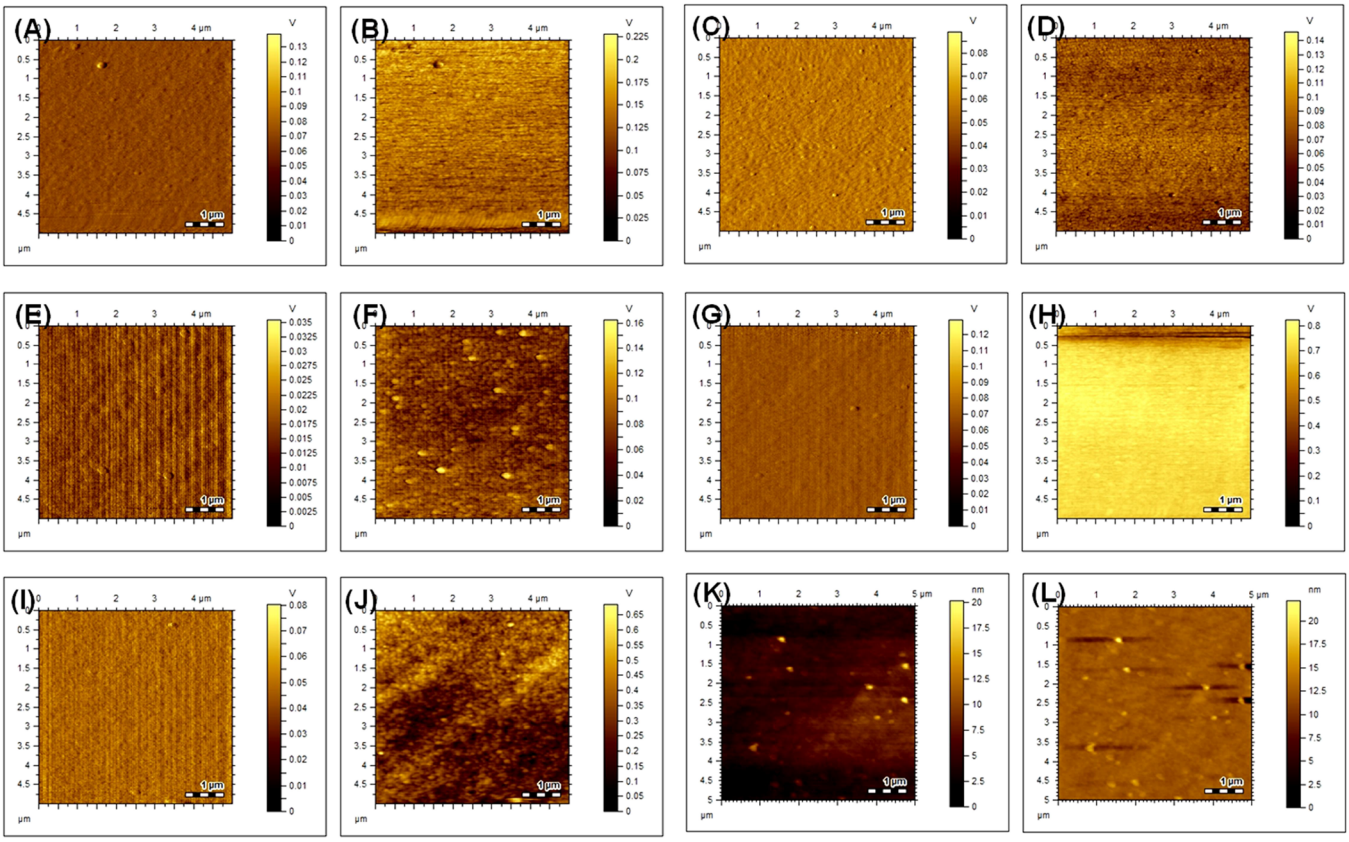

Figure 4. AFM images of OSCS before its loading with ACF (A and B) and after its loading (C and D) at pH 6−8. AFM images of OSCS before its loading with ACF (E and F) and after its loading (G and H) at pH 5. AFM images of OSCS before its loading with ACF (I and J) and after its loading (K and L) at pH 1.2.

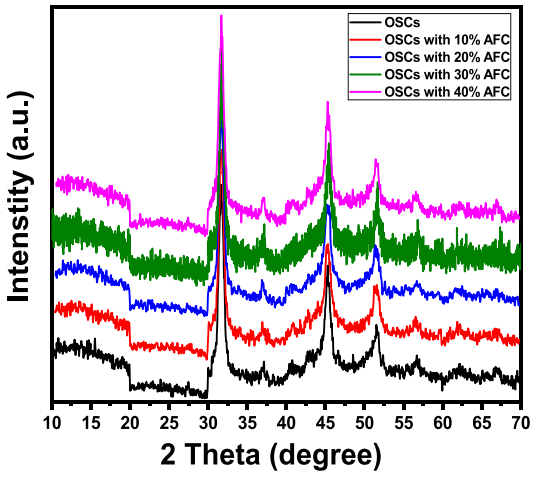

Figure 5. XRD patterns of OSCS and ACF-loaded PMs.

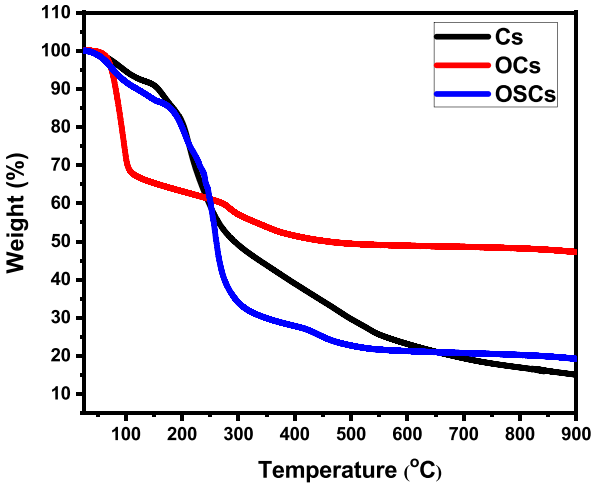

Figure 6. TGA thermograms of CS, OCS, and OSCS.

melting point of ACF, and the second was around 260 °C for the pH 5 sample (Figure 7D) and 280 °C for the pH 6−8 sample (Figure 7E), which correspond to their thermal decompositions. In this case, a little variation in decomposition peak temperatures for the ACF-loaded PMs can be seen, indicating an effective integration of ACF with OSCS and a moderate stabilizing impact owing to the presence of the ACF.[45]

2.5. EE and LC of ACF-Loaded PMs. The EE and LC of ACF-loaded PMs with different grafted hydrophobic moieties are shown in Tables 1 and 2. For the pH 6−8 and pH 5 samples, the findings showed that the evaporation technique had a high EE (52.4−80.3%) and LC (52.52−216.13). The pH 5 samples with an initial ACF/polymer ratio of 30% had the highest EE of 80.3% and LC of 216.13, while pH 1.2 showed the lowest EE of 13.3 to 15.3% and LC of 43.79 to 113.41, Therefore, the optimum ACF-loading ratio was 30% for pH 5 samples. This high concentration suggests that hydrophobic medicines have been successfully incorporated into polymeric self-assemblies with a strong water solubility. Micelle production and drug assimilation into the micelles were predicted to take place at the same time.[26] This inclusion

https://doi.org/10.1021/acsomega.3c07065
ACS Omega 2023, 8, 48145−48158

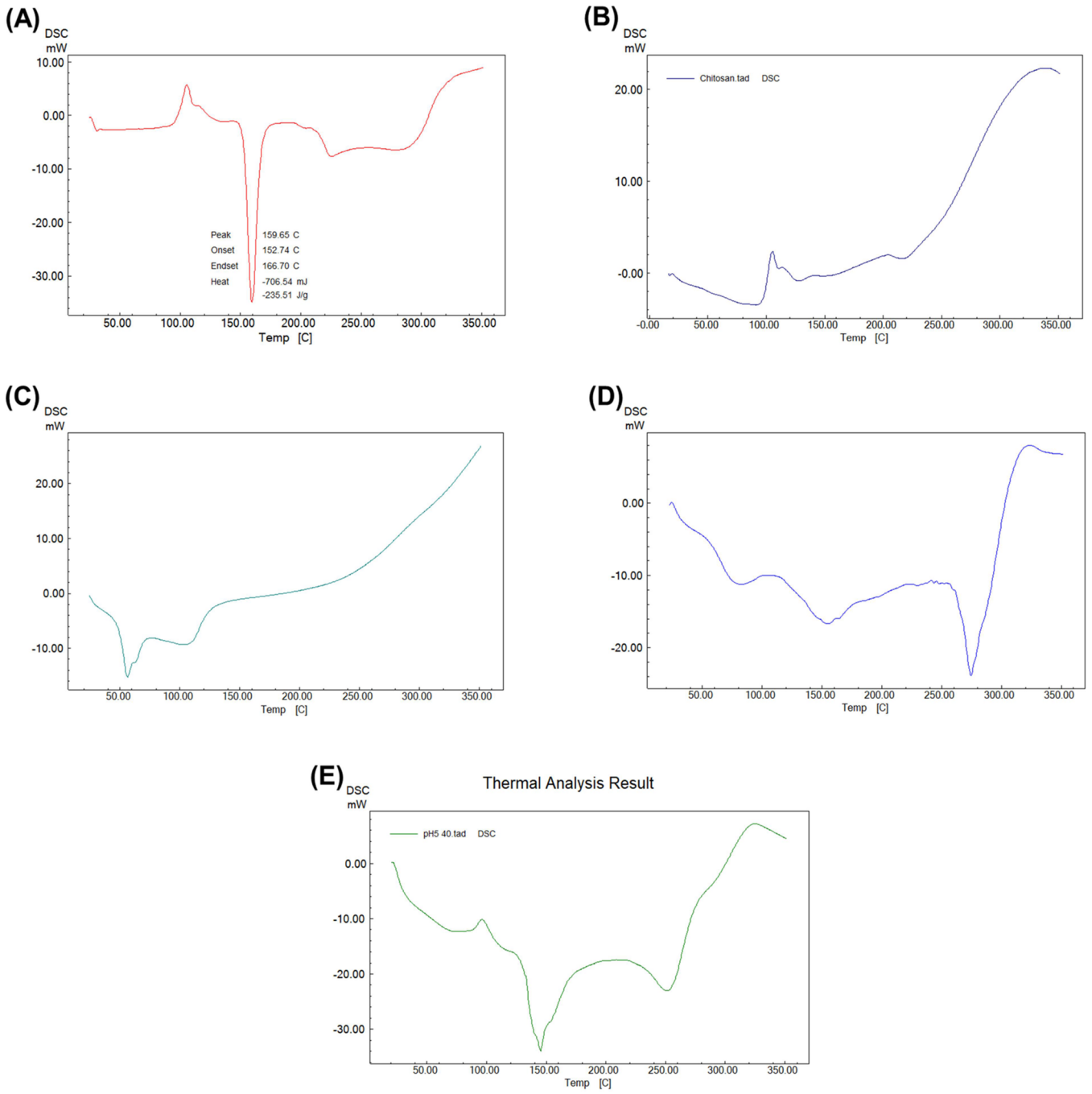

Figure 7. DSC spectrum of pure ACF (A), CS (B), OSCS (C), and ACF-loaded PMs for the pH 5 sample (D) and ACF-loaded PMs for the pH 6−8 sample (E).

process may be controlled by the hydrophobic contacts between the hydrophobic *N*-octyl CS chain, ACF, and the solvent. The drug-to-polymer weight ratios and hydrophobic moieties of the drug had a significant impact on EE and LC. This finding was consistent with prior research, which found that the drug's EE in the PMs was influenced by the technique of inclusion.[46] Pure ACF UV absorbance results are shown in Table 3, and their standard calibration curve is shown in Figure 8.

2.6. In Vitro ACF Release. Chitosan was soluble at a pH less than 7.0 due to the protonation of the amine group in the acidic medium. On the other hand, chitosan was insoluble in both neutral and basic media, attributed to the rigid crystalline structure of chitosan, which has a strong hydrogen bond. In contrast to chitosan, all *N*-octyl chitosan derivatives exhibited excellent solubility properties at pH values of 1.0 to 13.0.[47] The in vitro release behavior of ACF from a pure drug and ACF-loaded pH-responsive PMs is shown in Figure 9 and Table 4. The release studies were performed for 8 h to mimic the conditions of the GI tract. For the initial 2 h, 0.1 N HCl (pH 1.2) medium was used as the release medium to simulate the gastric fluid (SGF) medium of the stomach. During the next 6 h, the pH was adjusted to 6.8 to simulate the intestinal fluid (SIF) medium of the small intestine. At the end of 2 h, as shown in Figure 9 and Table 4, the amount of drug released from the pure drug and ACF-loaded PMs was 5.8 and 18.8%,

https://doi.org/10.1021/acsomega.3c07065
ACS Omega 2023, 8, 48145−48158

Table 1. Standard Calibration Curve for ACF in Different pH Media

sample	absorbance of pH 6−8 samples		absorbance of pH 5 samples		absorbance of pH 1.2 samples	
	conc. (μg/mL)	absorbance	conc. (μg/mL)	absorbance	conc. (μg/mL)	absorbance
1	0	0.0004	0	0.0002	0	0.0003
2	5	0.2039	5	0.1341	5	0.1528
3	10	0.3160	10	0.2794	10	0.3346
4	15	0.5382	15	0.4196	15	0.5992
5	20	0.5996	20	0.5874	20	0.7066
6	25	0.7413	25	0.7046	25	0.8358
7	30	0.9269	30	0.8713	30	1.0745
8	35	1.0749	35	0.9946	35	1.2379
9	40	1.2680	40	1.1798	40	1.334
10	45	1.3890	45	1.2953	45	1.516
11	50	1.5215	50	1.4202	50	1.9327

Table 2. EE of ACF-Loaded PMs

sample ACF (%)	EE of pH 6−8 samples (%)	EE of pH 5 samples (%)	EE of pH 1.2 samples (%)
10%	57.8	78.3	15.1
20%	65.5	65.9	15.3
30%	52.4	80.3	13.9
40%	40.2	75.7	13.3

Table 3. LC of ACF-Loaded PMs

sample ACF (%)	LC of pH 6−8 samples (μg/mg)	LC of pH 5 samples (μg/mg)	LC of pH 1.2 samples (μg/mg)
10%	52.52	71.22	43.79
20%	109.27	109.86	76.84
30%	121.02	185.36	101.05
40%	114.31	216.13	113.41

respectively. It is clear from the obtained results that, at all release points, the release of ACF was significantly enhanced by the prepared ACF-loaded PMs ($p < 0.05$). As the pH of the dissolution medium increased from 1.2 to 7.4, ACF showed a remarkable increase in the released amount from pure drug and from the prepared PMs. At the end of 3 h, the released amounts were 18.3 and 37.1% from pure drug and ACF-loaded PMs, respectively. At the end of the dissolution study, after 8 h, the released amounts were 5.6 and 94.1% from pure drug and ACF-loaded PMs, respectively. Again, it is clear from the obtained results that, at all release points, the release of ACF was significantly enhanced by the prepared ACF-loaded PMs ($p < 0.05$).

ACF has a weakly acidic nature and a pK_a value of 4.157 and is practically insoluble in the acidic medium; therefore, the release of ACF in 0.1 N HCl could hardly be noticed. With reference to the pH solubility profile, the dissolution rate of ACF has been shown to increase with the increasing pH of the medium. This theory justifies our observation that drug release was very slow in the acidic medium (pH 1.0) and subsequently increased at higher pH levels.[48] This supports the higher drug release in phosphate buffer (pH, 7.4) in the present study. There are several prominent factors related to the core that were identified to affect the drug release from pH-sensitive PMs, including hydrophobicity, rigidity of the core, hydrogen bonding, steric factors, and p−p interaction, which may limit water penetration into the inner core structures.[49] This indicated that the prepared pH-sensitive PMs could retain the ACF within the inner core of the PMs. It is important to note that the lower levels of ACF release in the SGF medium may be due to the poor solubility of ACF at an acidic pH. Also, the carboxyl groups in the succinic acid moiety of the self-assembled PMs were protonated at a low pH, resulting in a tight and rigid structure. In addition, the hydrophobic interactions between the octyl moieties in the chain and ACF increased as the acidity increased. When the pH was increased to 6.8, the ACF release dramatically increased.[50] This result is in agreement with the results obtained by Kamal Dua et al.[51] Upon dilution of the micelle solution to a very low concentration (typically $<10^{-3}$ mM), the surfactant content will not be sufficient to drive the self-assembly of micelles;, instead, they tend to distribute at the air−water or aqueous−organic solvent interface which leads to the disintegration of the micelles

2.7. In Vivo Anti-Inflammatory Study. Carrageenan-induced paw edema in rats is a well-established model of acute inflammation for the screening of anti-inflammatory agents. However, injection of carrageenan into the hind paw induced a progressive edema.[52] The results obtained are shown in Table 5 and Figure 9B,C. Results showed a significant increase in paw volume in the carrageenan control group (II) compared to that of the normal animals in group I (negative control) and also in other treated groups III and IV. The paw volume increased from 0.130 ± 0.006 mL at 0 h treatment to 0.835 ± 0.028 mL at 2 h treatment. The paw volume of group II showed its maximum at 4 h of treatment (1.333 ± 0.036 mL), and then it started to decrease (1.227 ± 0.026 mL) at 6 h of treatment. The paw volume of animals treated with standard ACF at 10 mg/kg (gp III) showed a significant ($p < 0.001$) reduction in paw volume at all time points during the experiment compared to the control group. The same trend was noticed in animals upon treatment with the prepared ACF-loaded PM group (IV). Treatment of animals with the formula showed a nonsignificant difference ($p > 0.05$) compared to the standard ACF group at 0, 1, and 2 h of treatment, while it showed a significant difference at 3 ($p < 0.05$), 4 ($p < 0.01$), and 6 h of treatment ($p < 0.001$). After 6 h of treatment, animals in GP (IV) showed a nonsignificant difference ($p > 0.05$) compared to the negative control group animals.

Table 6 and Figure 9D show the inhibition (%) of paw edema by different treatments. Treatment with standard ACF showed the inhibition of paw edema by 39.42 and 74.98% at 1 and 6 h, respectively. Treatment with ACF-loaded PMs showed the inhibition of paw edema by 40.87 and 85.09% at 1 and 6 h, respectively. As it is shown in the obtained results, ACF-loaded PMs showed a statistically significant ($p < 0.001$) reduction in paw volume compared to the standard ACF. At

https://doi.org/10.1021/acsomega.3c07065
ACS Omega 2023, 8, 48145−48158

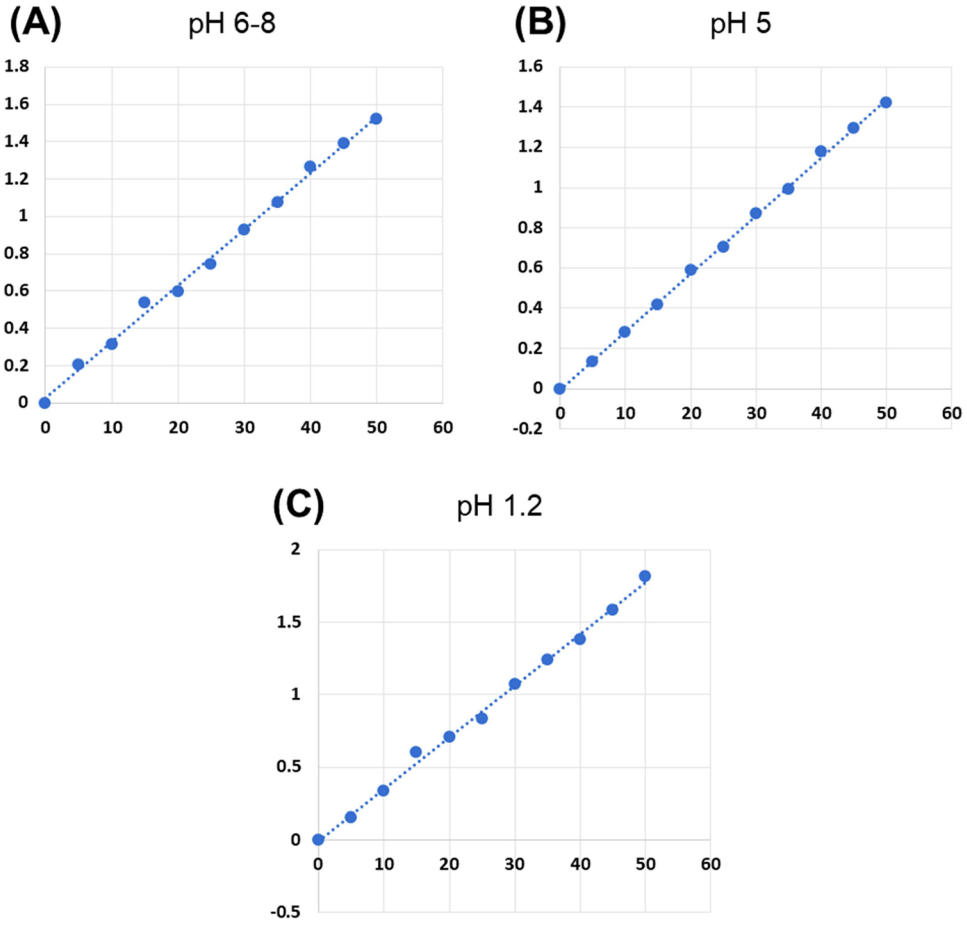

Figure 8. Standard calibration curve for ACF: (a) pH 6−8, (b) pH 5, and (c) pH 1.2.

the same time, results revealed that there is no significant difference ($p > 0.05$) between ACF-loaded PMs and the negative control group after 6 h of treatment.

The carrageenan-induced rat paw edema model is a suitable test for evaluating anti-inflammatory drugs and has been widely used as a reliable model to assess the antiedematous activity of various agents (Figure 10).[53,54] Induction of edema in rat paws by carrageenan involves the production or release of different biologically active mediators at the affected site. The released mediators include histamine, bradykinins, and leukotrienes in addition to prostaglandins, especially the E series. The development of edema induced by carrageenan is commonly correlated with a primary exudative stage of inflammation. The carrageenan-induced inflammation model is a highly predictive model for anti-inflammatory agents; therefore, the results of this test are significant indicators of the inflammatory activity. Although both the cyclooxygenase and lipoxygenase pathways play a crucial role in the progress of inflammatory procedures, suppression of the cyclooxygenase pathway is more effective in reducing carrageenan-induced inflammation than lipoxygenase pathway inhibition.[26] The formation of paw edema gradually increased within the first 1 h after carrageenan injection (Figure 11). Standard ACF (10 mg/kg) significantly ($p < 0.05$) decreased the paw edema at all experiment time points; similarly, the prepared ACF-loaded PMs caused a significant ($p < 0.001$) reduction of paw edema at all experiment time points. However, the prepared formula showed a significant difference ($p < 0.001$) compared to the standard ACF at 6 h of treatment, and it also showed a nonsignificant difference ($p > 0.05$) compared to the negative control group at 6 h of treatment.

3. CONCLUSIONS

A pH-responsive amphiphilic CS derivative, OSCS, was effectively synthesized and loaded with a weakly water-soluble medication (ACF) by using a physical entrapment technique (evaporation method) to form ACF-loaded PMs. The effective production of amphiphilic OSCS by the *N*-amination procedure, followed by an N,O-succinylation reaction is shown by ^{1}H NMR and FT-IR characterizations. TEM, DLS, and AFM findings supported the effective integration of ACF into PMs by the formation of a spherical morphology. The pH 5 sample with an ACF/polymer ratio of 30% had the highest ACF EE and LC and can be recommended as a potential oral medication delivery tool for ACF and similar hydrophobic drugs. The release profile of ACF-loaded pH-responsive PMs (94% after 480 min) is faster than the obtained behavior for free ACF (59.56% after 480 min), and the release rates increase significantly by raising the pH from 1.2 to 4.7. Based on the carrageenan-induced inflammation model of paw edema in rats, the ACF-loaded PMs (10 mg/kg) display enhanced inflammation activities as compared to free ACF at the same dosages and time intervals. However, the application of ACF-loaded PMs for 6 h resulted in inhibition effects on the paw edema by 85.09% as compared to 74.9% for the free ACF drug.

https://doi.org/10.1021/acsomega.3c07065
ACS Omega 2023, 8, 48145−48158

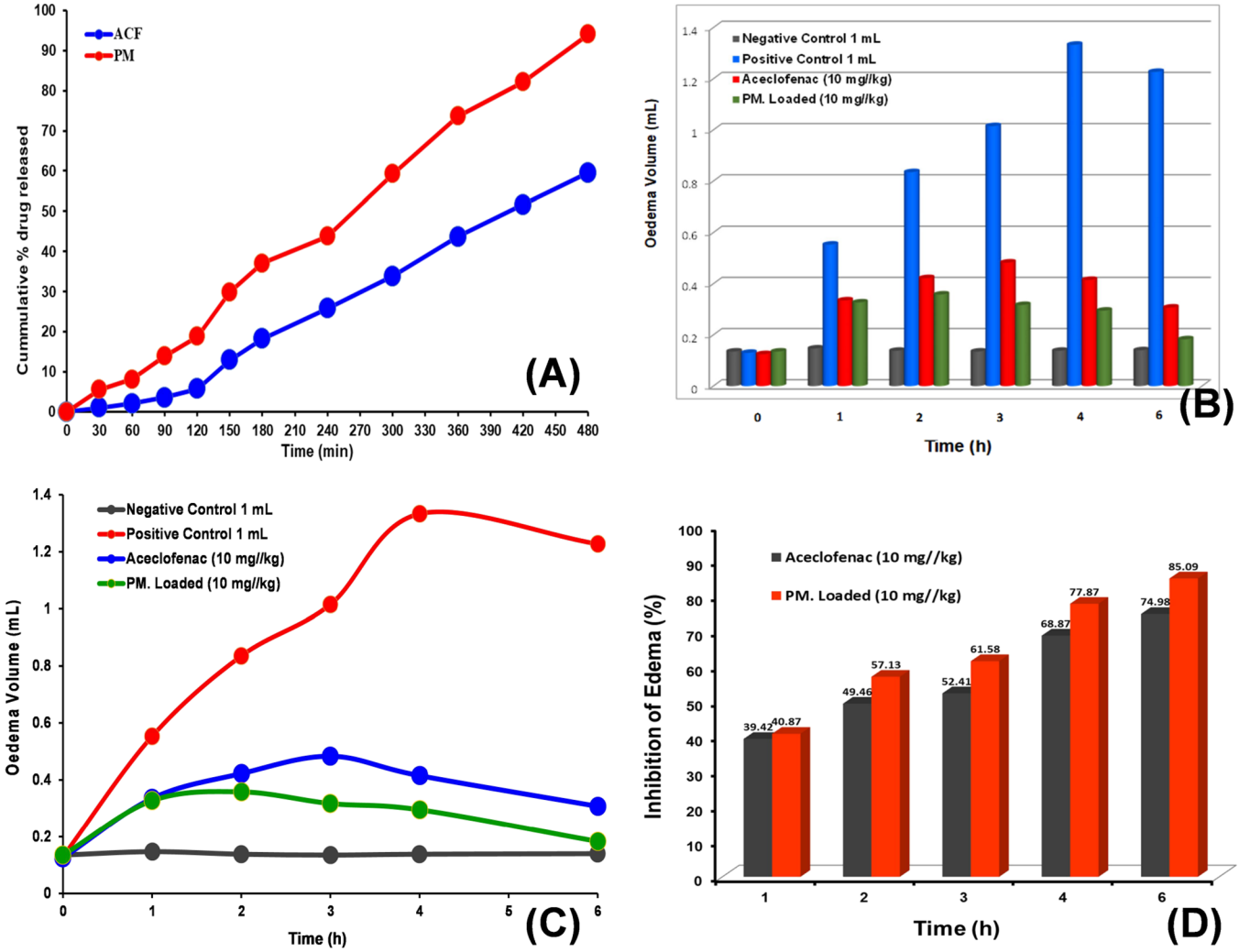

Figure 9. In vitro dissolution profiles of ACF and ACF-loaded PMs (A), effect of ACF and its loaded PMs on carrageenan-induced edema of hind paw in rats (B), effect of ACF and its loaded PMs on carrageenan-induced edema of hind paw in rats (C), and % inhibition of edema in rats by ACF and its loaded PMs on carrageenan-induced edema of hind paw in rats (D).

Table 4. In Vitro Dissolution Profiles of ACF and ACF-Loaded PMs

time (min)	ACF	PMs
0	0	0
30	1.1	5.6
60	2.1	8.2
90	3.6	13.9
120	5.8	18.8
150	13	29.9
180	18.3	37.1
240	25.8	43.8
300	33.9	59.3
360	43.7	73.6
420	51.6	82.1
480	59.6	94.1

4. MATERIALS AND METHODS

4.1. Materials. CS was purchased from BIOSYNTH Carbosynth Ltd. (Compton, United Kingdom). ACF was obtained from Livealth BioPharma Pvt., Ltd. (India). Octylaldehyde, benzaldehyde, ethanol, acetic acid, sodium hydroxide (NaOH), sodium borohydride ($NaBH_4$), *N*,*N*-dimethylformamide (DMF), dimethyl sulfoxide (DMSO), succinic anhydride, carrageenan, and carboxymethylcellulose sodium salt (Na-CMC) were purchased from Sigma-Aldrich Chemical Co. (St. Louis, MO, USA) and used without further treatment. The PH-211 microprocessor pH meter was purchased from Hanna Instruments in Washington, USA. Centrifuge MPW-251 from MPW Instruments (Warszawa, Poland) was used. Membrane filters of 0.45 m in diameter were purchased from ISOLAB Laborgeräte GmbH, Am Dillhof 2, 63863 Eschau, Germany.

4.2. Methods. *4.2.1. OSCS Synthesis.* Following a technique reported by Woraphatphadung et al.,[25] an *N*-amination reaction was followed by an N,O-succinylation reaction in order to produce OSCS. The first step involved dissolving 1.3102 mmol of CS in 150 mL of 1% aqueous acetic acid (v/v) and then adding 100 mL of ethanol to the mixture. The reaction mixture was stirred at room temperature for 24 h after the addition of octyl aldehyde (2.0 meq/GlcN). For the reduction step, 2.0 g of $NaBH_4$ (52.9 mmol) was added to the solution. Afterward, to bring the pH down to 5, NaOH (1 M) was added. For the next 24 h, the reaction mixture was stirred continuously at room temperature. Using filtration, the precipitate was collected, washed multiple times with ethanol,

https://doi.org/10.1021/acsomega.3c07065
ACS Omega 2023, 8, 48145−48158

Table 5. Inhibitory Effect of ACF and Its Loaded PMs on Carrageenan-Induced Edema of Hind Paw in Rats[a]

time (h)	0	1	2	3	4	6
negative control 1 mL	0.135 ± 0.006	0.147 ± 0.006	0.138 ± 0.009	0.135 ± 0.009	0.138 ± 0.005	0.140 ± 0.004
positive control 1 mL	0.130 ± 0.006	0.553 ± 0.037	0.835 ± 0.028	1.015 ± 0.037	1.333 ± 0.036	1.227 ± 0.026
ACF (10 mg/kg)	0.125 ± 0.006	0.335 ± 0.022	0.422 ± 0.014	0.483 ± 0.013	0.415 ± 0.024	0.307 ± 0.022
loaded PMs (10 mg/kg)	0.135 ± 0.008	0.327 ± 0.015	0.358 ± 0.017	0.317 ± 0.068	0.295 ± 0.019	0.183 ± 0.015

[a]Data represent mean values ± SEM (standard error of mean) of six rats per group. Statistical comparison of the difference between the saline control group and treated groups was done by one-way ANOVA (analysis of variance), *$p < 0.0001$.

Table 6. Inhibition (%) of Edema in Rats by ACF and Its Loaded PMs on Carrageenan-Induced Edema of Hind Paw in Rats

	inhibition (%) of rat paw edema				
time (h)	1	2	3	4	6
ACF (10 mg/kg)	39.42	49.46	52.41	68.87	74.98
ACF-loaded PMs (10 mg/kg)	40.87	57.13	61.58	77.87	85.09

Figure 10. Photograph of the plethysmometer used for carrageenan-induced edema of hind paw in rats.

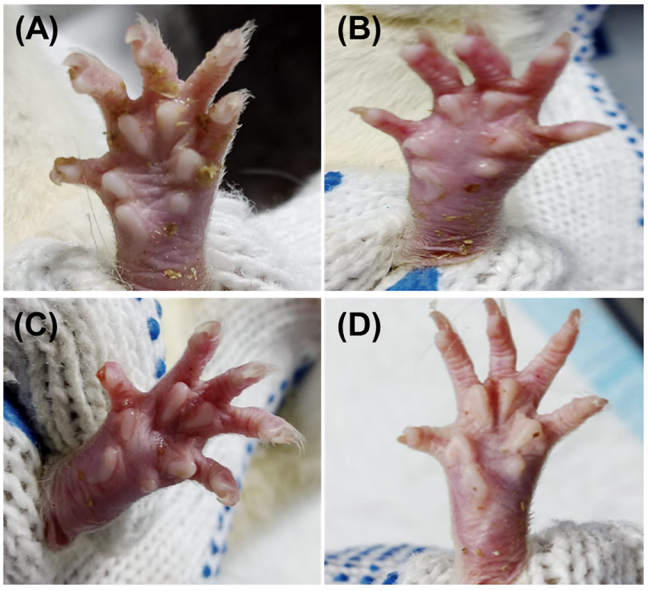

Figure 11. Photograph of the carrageenan-induced rat paw edema after 3 h; (A) control negative, (B) control positive, (C) ACF (10 mg/kg), and (D) ACF-loaded PM (10 mg/kg).

and then dried under vacuum at room temperature. N-octyl CS derivatives (OCS) were produced in this step.

The second step, which is the *N*,*O*-succinylation of OCS, was carried out using succinic anhydride. After dissolving 4.6 mmol of dried OCS in 40 mL of DMF/DMSO (1:1), 3.0 g of succinic anhydride (5.0 meq/GlcN) was added, and the mixture was stirred for 24 h. The reaction was maintained at 100 °C in a nitrogen environment. After cooling it to room temperature, the reaction mixture was filtered to eliminate any remaining undissolved OCS. To remove excess succinic anhydride and DMF, the clear solution was dialyzed with distilled water for 3 days before being oven-dried for 24 h at 80 °C. The powdered OSCS was then obtained (Figure 12). The theoretical molecular weight increases of the OCS and OSCS and the degree of substitution were used to calculate Mn of the derivatives.

4.2.2. Preparation of ACF-Loaded PMs. The mixed-solvent evaporation process described by Woraphatphadung et al.[6] was used to create the PMs. In short, DMF was used to dissolve 10 mg of OSCS derivatives and ACF (0−40%, w/w to polymers) in a glass-bottomed container. The solution was mixed with acetone (1/3 of DMF) and stirred at room temperature under a nitrogen atmosphere until the solvent was entirely evaporated. The solution was then sonicated at 80 °C for 20 min after adding 3 mL of distilled water, 1 M NaOH pH 5, or pH 1.2 acetic acid (Table 7). The obtained solution was centrifuged at 1000 rpm for 2 min. A membrane filter of 0.45 m in diameter was used to filter the solution, which was then collected in a 1 mL test tube centrifuge vial.

A UV−vis spectrophotometer (8453E, Santa Clara, CA, USA) at 273 nm was used to measure the EE and LC of ACF-PMs. ACF-PMs were dissolved in a DMSO:H_2O (9:1 v/v) solution. A pure ACF calibration curve was used to determine the quantity of ACF loaded. To estimate the EE and LC values for ACF, we used eqs 1 and 2 accordingly. All samples were tested three times.

$$\mathrm{EE}(\%) = \frac{\text{Amount of ACF loaded into PMs}}{\text{Initial amount of ACF used for preparation}} \times 100 \quad (1)$$

$$\mathrm{LC}(\mu g/mg) = \frac{\text{Amount of ACF loaded into PMs}}{\text{Amount of amphiphilic OSCS used for preparation}} \quad (2)$$

4.2.3. Preparation of Dried ACF-PM Powder Samples. A volume of 15 mL of OSCS and ACF-loaded PMs was dried for 24 h in a freeze-dryer (Christ alpha 2−4 LDplus, Osterode am Harz, Germany). When the drying procedure was finished, the residue was collected in a 5 mL sample container and used for further studies.

4.3. Characterization of ACF-Loaded PMs. *4.3.1. Amphiphilic OSCS Characterization by ^{1}H NMR and FT-IR*

https://doi.org/10.1021/acsomega.3c07065
ACS Omega 2023, 8, 48145−48158

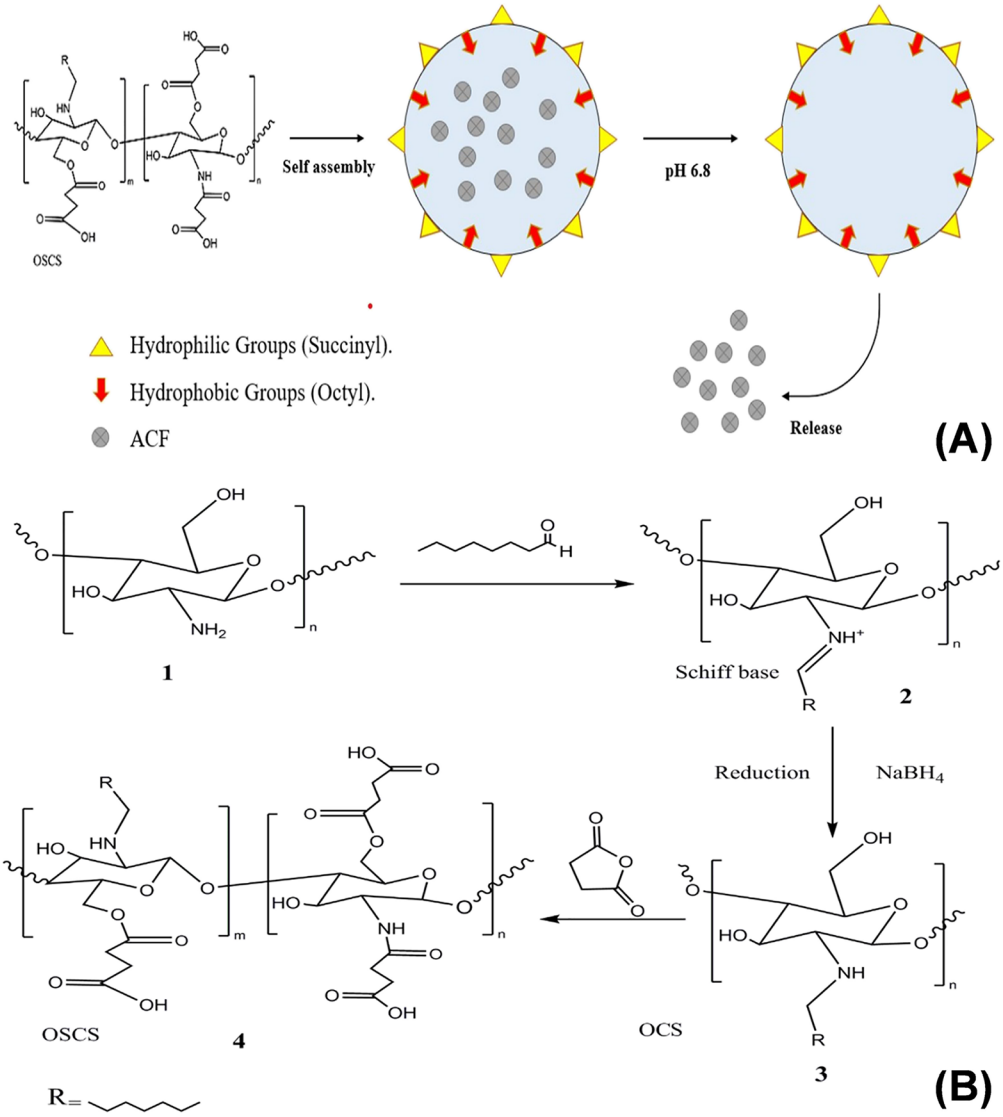

Figure 12. ACF loading into the inner core of PMs (OSCS) (A) and schematic diagram for the synthesis of OSCS by *N*-amination reaction, followed by *N,O*-succinylation reaction (B).

Table 7. Preparation of ACF-Loaded PMs with Different Percentages of ACF in Relation to the Constant Concentration of OSCS in Solvents with Different pH

OSCS	solvents	ACF percentage
10 mg	pH 6−8	0%
		10%
		20%
		30%
		40%
10 mg	pH 5	0%
		10%
		20%
		30%
		40%
10 mg	pH 1.2	0%
		10%
		20%
		30%
		40%

Analyses. ^{1}H NMR spectroscopy and FT-IR spectra were used to confirm the structures of CS, OCS, OSCS, and ACF-loaded PMs. 1H-NMR spectroscopy (JEOL RESONANCE spectrometer ECX-500 II) was used. For dilution, dimethyl sulfoxide-d6 (DMSO-d6) was employed as the solvent, and the 1H-NMR spectra were recorded at 297.15 K. The FT-IR analysis was obtained with a range of 4000−450 cm^{-1} wavenumbers using a FT-IR spectrometer with a module number (Nicolet 6700, purchased from Thermo-Electron Corporation, USA), using the OPUS Version 6.5 operation system.

4.3.2. AFM Analysis. An AFM system (AFM 5600LS, Agilent, Santa Clara, California) was utilized to get insights into the morphology and obtain 2D and 3D AFM images of OSCS and ACF-loaded PM samples. The samples were first exposed to ultrasonic waves for 1 h at a frequency of 60 kHz with an amplitude of 85% and 0.6 cycles (UP400S manufactured by Hielscher, Teltow, Germany); finally, a thin film was created using a coater instrument model Laurell-650Sz from Spain at a speed of 700 rpm under vacuum. Using contact mode, Al tap, 0.71 In/S speed, I. gain 2 and P. gain 4,

https://doi.org/10.1021/acsomega.3c07065
ACS Omega 2023, 8, 48145−48158

AFM pictures and data pro 30 le for 200 nm × 200 nm and its zoom 100 nm × 100 nm were obtained.

4.3.3. TEM Analysis. OSCS and ACF-loaded PM samples were also subjected to TEM. OSCS and ACF-loaded PM samples were sonicated for 50 min at an amplitude of 85% and 0.65 cycles at a frequency of 50 kHz using an ultrasonic instrument of 50 kHz (UP400S, Hielscher, Germany). A TEM-2100 high-resolution electron microscope (JEOL, Akishima, Tokyo 196−8558, Japan) was used to conduct TEM studies.

4.3.4. DLS Analysis. The average particle diameter and size distribution (PDI) of the produced OSCS and ACF-loaded PMs samples were measured using DLS (Malvern Instruments Ltd., Kassel, Germany, model NS500). A 0.45 mm membrane filter was used to filter the PM samples after they had been diluted with distilled water.

4.3.5. X-ray Diffraction (XRD) Analysis. Dried samples were used to validate the PM nanoparticle identification with an XRD instrument (XMD-300 from Unisantis Europe GmbH, Georgsmarienhütte, Germany). Diffraction data were collected using XQ Suite software.

4.3.6. Thermal Analysis. Tests for heat stability were carried out on ACF, CS, OCS, OSCS, and ACF-loaded PMs using TGA and DSC. TGA of CS, OCS, and OSCS was performed using a PerkinElmer Model TGA-7 thermogravimetric system. The mass of the polymers was in the range of 3 mg. The sample dish was placed in the balance system equipment with a heating rate of 10 °C/min and under nitrogen flow, in which the temperature was raised from 25 to 900 °C. The DSC experiment was carried out using a DSC-60 system (ShIMADZU Scientific Instruments, Kyoto, Japan). In aluminum cups and seals, we compressed dried samples of ACF, CS, and OSCS and different concentrations of ACF-loaded PMs. A heating rate of 10 °C per minute was used to record calorimetric curves in the range of 25−400 °C for the DSC examination of the films using TA-60 WS Collection Monitor Software.

4.3.7. In Vitro ACF Release. The in vitro drug release characteristics of ACF from selected prepared ACF-loaded PMs and free drugs were measured using the dialysis membrane method under sink conditions.[6] Here, approximately 5 mg of pure ACF and an equivalent amount of ACF in ACF-loaded PMs were dissolved in 3 mL of PBS solution (0.1 M, pH 7.4) and then subsequently placed in a dialysis bag (Spectra/Por 6 membrane, prewetted RC tubing, USA, MWCO 14,000 Da and diameter of 29 mm) and immersed in a beaker containing 250 mL of SGF medium (0.1 N HCl, pH 1.2) as a dissolution medium. The dissolution medium was maintained under constant continuous stirring at 100 rpm at room temperature for 2 h, and then, the pH of the medium was increased to 6.8 (SIF) with trisodium phosphate for 6 h. At predetermined intervals, 1 mL aliquots of the medium were withdrawn and replaced with an equal volume of the fresh medium. The aliquots were filtered through 0.45 mm membrane filters and analyzed spectrophotometrically at 273 nm. The release study for each sample was performed in three replicates.

4.3.8. In Vivo Evaluation of Anti-inflammatory Activity.

4.3.8.1. Animals and Treatment. Twenty-four healthy adult albino rats (130−150 g) of either sex were obtained from the animal house of Umm Al-Qura University, Makkah. Animals were housed in the animal house, Faculty of Pharmacy, fed with commercially available feed, and maintained under standard conditions of temperature (25 °C ± 5 °C), relative humidity (55 ± 10%), and 12/12 h light/dark cycle. They were allowed free access to a standard dry pellet diet and water ad libitum. Animals were acclimatized for a period of 1 week before starting the experimental procedures. All treatments included ACF and ACF-loaded PMs that were prepared as suspensions in 0.5% Na-CMC.

4.3.8.2. Carrageenan-Induced Rat Paw Edema Model. The in vivo anti-inflammatory activity of ACF and the prepared ACF-loaded PM formula was evaluated by the carrageenan-induced paw edema model. It was chosen because it is a sensitive and reproducible in vivo test for NSAID drugs and has long been established as a valid model for studying new anti-inflammatory drugs.[54] After overnight fasting, the rats were randomly divided into four groups, each containing six rats. Group I served as the negative control, which received only the vehicle (0.5% CMC in distilled water) and was administered orally (2 mL/kg); group II acted as the positive control, which received only the vehicle (0.5% CMC in distilled water); groups III and IV received orally a single dose of ACF (10 mg/kg body weight) and ACF-loaded PMs equivalent to 10 mg/kg, respectively.[55] The total volume of the oral dose was kept constant at 1 mL/rat.

Acute inflammation was induced by the subplantar administration of 0.1 mL of 1% freshly prepared λ carrageenan solution in normal saline in the left paw of rats; carrageenan administration was 30 min after the oral treatment of animals in groups II, III, and IV, while animals in group I were injected with an equal volume of normal saline. A colored mark was made on both the hind limbs at the tibio-tarsal joint.[56,57] The paw volume was measured just before the carrageenan injection, that is, at ″0 h", and then at 1, 2, 3, 4, and 6 h after the carrageenan injection using a plethysmometer (Ugo Basile, Comerio, Italy), where the paw edema volume was measured according to the water displacement method. In this method, the hind limb was dipped inside the tube up to the given mark, which caused water to overflow from the side outlet to the microburette. The displaced water volume was equal to the volume of the paw. Increases in the volume of the left hind paws were taken as an indication of paw edema. Edema was assessed in terms of the difference in the zero-time volume of the injected hind paw and its volume at time following carrageenan administration (i.e., 60, 120, 180, 240 min). Further, the percentage of inhibition of paw edema activity was calculated for each animal using equation 3:

$$\%\text{Inhibition} = \frac{\text{Vc(in milliliter} - \text{Vt(in milliliter)}}{\text{Vc(in milliliter)}} \times 100 \quad (3)$$

where Vc is the mean volume of paw edema in the control group of animals, and Vt is the mean volume of paw edema in the drug-treated group of animals.[58,59]

4.3.8.3. Statistical Analysis. The results are expressed as mean ± standard error of the mean (SEM). Comparisons between the experimental and control groups were performed by one-way ANOVA, followed by the Tukey−Kramer test. A value of $p < 0.05$ was considered a statistically significant result. The program used for the statistical analysis was GraphPad Prism software 5 (San Diego, CA, USA).

https://doi.org/10.1021/acsomega.3c07065
ACS Omega 2023, 8, 48145−48158

■ ASSOCIATED CONTENT

Supporting Information

The Supporting Information is available free of charge at https://pubs.acs.org/doi/10.1021/acsomega.3c07065.

XRD patterns of CS and ACF (PDF)

■ AUTHOR INFORMATION

Corresponding Author

Noof A. Alenazi − *Department of Chemistry, College of Science and Humanities in Al-Kharj, Prince Sattam bin Abdulaziz University, Al-Kharj 11942, Saudi Arabia;* orcid.org/0000-0002-8686-9203; Email: na.alenazi@psau.edu.sa

Authors

Mohammed G. Bokhari − *Department of Pharmaceutical Chemistry, Faculty of Pharmacy, Umm Al-Qura University, Makkah 21955, Saudi Arabia; First Medical Zone, Al-Madinah Health Cluster, Ministry of Health, Riyadh 11176, Saudi Arabia*

Mohammed A.S. Abourehab − *Department of Pharmaceutics, Faculty of Pharmacy, Umm Al-Qura University, Makkah 21955, Saudi Arabia*

Mostafa R. Abukhadra − *Materials Technologies and their Applications Lab, Geology Department, Faculty of Science, Beni-Suef University, Beni-Suef City 62511, Egypt; Geology Department, Faculty of Science, Beni-Suef University, Beni-Suef city 62511, Egypt;* orcid.org/0000-0001-5404-7996

Complete contact information is available at: https://pubs.acs.org/10.1021/acsomega.3c07065

Author Contributions

This article was written through the contributions of all authors. All authors have given approval to the final version of the manuscript.

Notes

The authors declare no competing financial interest.

■ ACKNOWLEDGMENTS

This study was supported via funding from Prince sattam bin Abdulaziz University project number (PSAU/2023/R/1445).

■ ABBREVIATIONS:

CS, Chitosan; ACF, Aceclofenac; NSAID, Nonsteroidal anti-inflammatory drug; COX-2, Cyclooxygenase-2; OSCS, *N*-octyl-*N*,*O*-succinyl CS; PMs, Polymeric micelles; AFM, Atomic force microscopy; TEM, Transmission electron microscopy; DLS, Dynamic light scattering; LC, Loading capacity; EE, Entrapment efficiency; NMR, Nuclear magnetic resonance; FT-IR, Fourier transform Infrared; DMF, Dimethylformamide; DMSO, Dimethyl sulfoxide; OCS, *N*-octyl CS derivatives; XRD, X-ray diffraction

■ REFERENCES

(1) Aranaz, I.; Harris, R.; Heras, A. Chitosan amphiphilic derivatives Chemistry and applications. *Current Organic Chemistry* **2010**, *14*, 308−330.

(2) Khan, T. A.; Peh, K. K.; Ch'ng, H. S. Reporting degree of deacetylation values of chitosan: the influence of analytical methods. *J. Pharm. Pharmaceut. Sci.* **2002**, *5*, 205−212.

(3) Croisier, F.; Jérôme, C. Chitosan-based biomaterials for tissue engineering. *European polymer journal* **2013**, *49*, 780−792.

(4) Raafat, D.; Sahl, H. Chitosan and its antimicrobial potential−a critical literature survey. *Microbial biotechnology* **2009**, *2*, 186−201.

(5) Bellich, B.; D'Agostino, I.; Semeraro, S.; Gamini, A.; Cesàro, A. "The good, the bad and the ugly" of chitosans. *Marine drugs* **2016**, *14*, 99.

(6) Woraphatphadung, T.; Sajomsang, W.; Gonil, P.; Treetong, A.; Akkaramongkolporn, P.; Ngawhirunpat, T.; Opanasopit, P. pH-Responsive polymeric micelles based on amphiphilic chitosan derivatives: Effect of hydrophobic cores on oral meloxicam delivery. *Int. J. Pharm.* **2016**, *497*, 150−160.

(7) Jiménez-Gómez, C. P.; Cecilia, J. A. Chitosan: a natural biopolymer with a wide and varied range of applications. *Molecules* **2020**, *25*, 3981.

(8) Kumar, S.; Mukherjee, A.; Dutta, J. Chitosan based nanocomposite films and coatings: Emerging antimicrobial food packaging alternatives. *Trends Food Sci. Technol.* **2020**, *97*, 196−209.

(9) Yilmaz Atay, H. *Antibacterial activity of chitosan-based systems; Functional chitosan*; Springer, 2019; pp 457−489.

(10) Chung, Y.; Su, Y.; Chen, C.; Jia, G.; Wang, H.; Wu, J. G.; Lin, J. Relationship between antibacterial activity of chitosan and surface characteristics of cell wall. *Acta Pharmacol. Sin.* **2004**, *25*, 932−936.

(11) Martins, A. F.; Facchi, S. P.; Follmann, H. D.; Pereira, A. G.; Rubira, A. F.; Muniz, E. C. Antimicrobial activity of chitosan derivatives containing N-quaternized moieties in its backbone: a review. *International Journal of Molecular Sciences* **2014**, *15*, 20800−20832.

(12) Ardean, C.; Davidescu, C. M.; Nemeş, N. S.; Negrea, A.; Ciopec, M.; Duteanu, N.; Negrea, P.; Duda-Seiman, D.; Musta, V. Factors influencing the antibacterial activity of chitosan and chitosan modified by functionalization. *International Journal of Molecular Sciences* **2021**, *22*, 7449.

(13) Rahimi, M.; Ahmadi, R.; Kafil, H. S.; Shafiei-Irannejad, V. A novel bioactive quaternized chitosan and its silver-containing nanocomposites as a potent antimicrobial wound dressing: Structural and biological properties. *Mater. Sci. Eng., C* **2019**, *101*, 360−369.

(14) Sharma, D.; Singh, J. Synthesis and characterization of fatty acid grafted chitosan polymer and their nanomicelles for nonviral gene delivery applications. *Bioconjug Chem* **2017**, *28* (11), 2772−2783.

(15) Tomadoni, B.; Ponce, A.; Pereda, M.; Ansorena, M. R. Vanillin as a natural cross-linking agent in chitosan-based films: Optimizing formulation by response surface methodology. *Polym Test.* **2019**, *78*, No. 105935.

(16) Garg, U.; Chauhan, S.; Nagaich, U.; Jain, N. Current advances in chitosan nanoparticles based drug delivery and targeting. *Advanced pharmaceutical bulletin* **2019**, *9* (2), 195.

(17) Balde, A.; Kim, S. K.; Abdul, N. R. Crab (Charybdis natator) exoskeleton derived chitosan nanoparticles for the in vivo delivery of poorly water-soluble drug: Ibuprofen. *International Journal of Biological Macromolecules* **2022**, *212*, 283−293.

(18) Wang, Y.; Pang, X.; Luo, J.; Wen, Q.; Wu, Z.; Ding, Q.; Zhao, L.; Yang, L.; Wang, B.; Fu, S. Naproxen nanoparticle-loaded thermosensitive chitosan hydrogel for prevention of postoperative adhesions. *ACS Biomaterials Science & Engineering* **2019**, *5* (3), 1580−1588.

(19) Dooley, M.; Spencer, C. M.; Dunn, C. J. *Aceclofenac. Drugs* **2001**, *61*, 1351−1378.

(20) Koirala, S.; Nepal, P.; Ghimire, G.; Basnet, R.; Rawat, I.; Dahal, A.; Pandey, J.; Parajuli-Baral, K. Formulation and evaluation of mucoadhesive buccal tablets of aceclofenac. *Heliyon* **2021**, *7*, No. e06439.

(21) Qin, L.; Jing, G.; Cui, N.; Xu, Z.; He, Y.; Qin, Y.; Lu, T.; Sun, J.; Du, A.; Wang, S. Resveratrol-silica aerogel nanodrug complex system enhances the treatment of sports osteoarthritis by activating SIRT-1. *Adv. Compos. Hybrid Mater.* **2023**, *6* (1), 3.

(22) Zhang, S.; Hou, Y.; Chen, H.; Liao, Z.; Chen, J.; Xu, B. B.; Kong, J. Reduction-responsive amphiphilic star copolymers with long-chain hyperbranched poly (ε-caprolactone) core and disulfide bonds for trigger release of anticancer drugs. *Eur. Polym. J.* **2018**, *108*, 364−372.

(23) Qu, D.; Jiao, M.; Lin, H.; Tian, C.; Qu, G.; Xue, J.; Xue, L.; Ju, C.; Zhang, C. Anisamide-functionalized pH-responsive amphiphilic chitosan-based paclitaxel micelles for sigma-1 receptor targeted prostate cancer treatment. *Carbohydr. Polym.* **2020**, *229*, No. 115498.
(24) Bai, T.; Shao, D.; Chen, J.; Li, Y.; Xu, B. B.; Kong, J. pH-responsive dithiomaleimide-amphiphilic block copolymer for drug delivery and cellular imaging. *Journal of colloid and interface science* **2019**, *552*, 439−447.
(25) Woraphatphadung, T.; Sajomsang, W.; Gonil, P.; Saesoo, S.; Opanasopit, P. Synthesis and characterization of pH-responsive N-naphthyl-N, O-succinyl chitosan micelles for oral meloxicam delivery. *Carbohydr. Polym.* **2015**, *121*, 99−106.
(26) Liu, Y.; Sun, Y.; He, S.; Zhu, Y.; Ao, M.; Li, J.; Cao, Y. Synthesis and characterization of gibberellin−chitosan conjugate for controlled-release applications. *Int. J. Biol. Macromol.* **2013**, *57*, 213−217.
(27) Kajjari, P. B.; Manjeshwar, L. S.; Aminabhavi, T. M. Novel blend microspheres of poly (vinyl alcohol) and succinyl chitosan for controlled release of nifedipine. *Polymer bulletin* **2013**, *70*, 3387−3406.
(28) Jain, N.; Rajoriya, V.; Jain, P. K.; Jain, A. K. Lactosaminated-N-succinyl chitosan nanoparticles for hepatocyte-targeted delivery of acyclovir. *J. Nanoparticle Res.* **2014**, *16*, 2136.
(29) Pestov, A.; Nazirov, A.; Modin, E.; Mironenko, A.; Bratskaya, S. Mechanism of Au (III) reduction by chitosan: Comprehensive study with 13C and 1H NMR analysis of chitosan degradation products. *Carbohydr. Polym.* **2015**, *117*, 70−77.
(30) Jaidee, A.; Rachtanapun, P.; Luangkamin, S. In In 1H-NMR analysis of degree of substitution in N, O-carboxymethyl chitosans from various chitosan sources and types; Advanced Materials Research. *Trans Tech Publ* **2012**, *506*, 158−161.
(31) Zhang, C.; Qineng, P.; Zhang, H. Self-assembly and characterization of paclitaxel-loaded N-octyl-O-sulfate chitosan micellar system. *Colloids and Surfaces B: Biointerfaces* **2004**, *39*, 69−75.
(32) Kamari, A.; Yusoff, S. N. M. N-octyl chitosan derivatives as amphiphilic carrier agents for herbicide formulations. *Open Chemistry* **2019**, *17*, 365−380.
(33) Kumar, R.; Kulkarni, A.; Nagesha, D. K.; Sridhar, S. In vitro evaluation of theranostic polymeric micelles for imaging and drug delivery in cancer. *Theranostics* **2012**, *2*, 714.
(34) Liang, N.; Sun, S.; Gong, X.; Li, Q.; Yan, P.; Cui, F. Polymeric micelles based on modified glycol chitosan for paclitaxel delivery: Preparation, characterization and evaluation. *International journal of molecular sciences* **2018**, *19*, 1550.
(35) Yang, J. S.; Zhou, Q. Q.; He, W. Amphipathicity and self-assembly behavior of amphiphilic alginate esters. *Carbohydr. Polym.* **2013**, *92*, 223−227.
(36) Woraphatphadung, T.; Sajomsang, W.; Rojanarata, T.; Ngawhirunpat, T.; Tonglairoum, P.; Opanasopit, P. Development of chitosan-based pH-sensitive polymeric micelles containing curcumin for colon-targeted drug delivery. *AAPS PharmSciTech* **2018**, *19*, 991−1000.
(37) Zhu, Y.; Chen, F. pH-responsive drug-delivery systems. *Chem. − Asian J.* **2015**, *10*, 284−305.
(38) Tonglairoum, P.; Woraphatphadung, T.; Ngawhirunpat, T.; Rojanarata, T.; Akkaramongkolporn, P.; Sajomsang, W.; Opanasopit, P. Development and evaluation of N-naphthyl-N, O-succinyl chitosan micelles containing clotrimazole for oral candidiasis treatment. *Pharm. Dev. Technol.* **2017**, *22*, 184−190.
(39) Roldo, M.; Power, K.; Smith, J. R.; Cox, P. A.; Papagelis, K.; Bouropoulos, N.; Fatouros, D. G. N-Octyl-O-sulfate chitosan stabilises single wall carbon nanotubes in aqueous media and bestows biocompatibility. *Nanoscale* **2009**, *1*, 366−373.
(40) Wu, J.; Zhong, F.; Li, Y.; Shoemaker, C. F.; Xia, W. Preparation and characterization of pullulan−chitosan and pullulan−carboxymethyl chitosan blended films. *Food Hydrocoll.* **2013**, *30*, 82−91.
(41) Li, A.; Xue, Q.; Ye, Y.; Gong, P.; Deng, M.; Jiang, B. Study on TEMPO-mediated oxidation of N-succinyl chitosan and the water retention property. *Molecules* **2020**, *25*, 4698.
(42) Vadher, A. H.; Parikh, J. R.; Parikh, R. H.; Solanki, A. B. Preparation and characterization of co-grinded mixtures of aceclofenac and Neusilin US2 for dissolution enhancement of aceclofenac. *AAPS PharmSciTech* **2009**, *10*, 606−614.
(43) Li, L.; Liang, N.; Wang, D.; Yan, P.; Kawashima, Y.; Cui, F.; Sun, S. Amphiphilic polymeric micelles based on deoxycholic acid and folic acid modified chitosan for the delivery of paclitaxel. *International journal of molecular sciences* **2018**, *19*, 3132.
(44) Jain, N.; Rajoriya, V.; Jain, P. K.; Jain, A. K. Lactosaminated-N-succinyl chitosan nanoparticles for hepatocyte-targeted delivery of acyclovir. *J. Nanoparticle Res.* **2014**, *16*, 2136.
(45) Zhang, C.; Ding, Y. A.; Ping, Q.; Yu, L. Novel chitosan-derived nanomaterials and their micelle-forming properties. *J. Agric. Food Chem.* **2006**, *54*, 8409−8416.
(46) Sripetthong, S. *Development of Curcumin Analog Nanopolymeric Micelle Delivery System using N-benzyl-NO-succinyl Chitosan for Anticancer Improvement*, 2019.
(47) Miele, D.; Catenacci, L.; Sorrenti, M.; Rossi, S.; Sandri, G.; Malavasi, L.; Dacarro, G.; Ferrari, F.; Bonferoni, M. C. Chitosan oleate coated poly lactic-glycolic acid (PLGA) nanoparticles versus chitosan oleate self-assembled polymeric micelles, loaded with resveratrol. *Marine drugs* **2019**, *17*, 515.
(48) Daman, Z.; Ostad, S.; Amini, M.; Gilani, K. Preparation, optimization and in vitro characterization of stearoyl-gemcitabine polymeric micelles: a comparison with its self-assembled nanoparticles. *Int. J. Pharm.* **2014**, *468*, 142−151.
(49) Quiñones, J. P.; Gothelf, K. V.; Kjems, J.; Caballero, Á M. H.; Schmidt, C.; Covas, C. P. Self-assembled nanoparticles of glycol chitosan−ergocalciferol succinate conjugate, for controlled release. *Carbohydr. Polym.* **2012**, *88*, 1373−1377.
(50) Yassin, H. A.; Ibrahim, M. A.; Abou-Taleb, H. A. Aceclofenac-Loaded Microspheres Prepared by Vesicular Ionotropic Gelation to Minimize Drug-induced Gastric Ulcers in Rats. *Curr. Drug Metab.* **2022**, *23*, 329−338.
(51) Yokoyama, M. Polymeric micelles as drug carriers: their lights and shadows. *J. Drug Target.* **2014**, *22*, 576−583.
(52) Samprasit, W.; Akkaramongkolporn, P.; Ngawhirunpat, T.; Rojanarata, T.; Opanasopit, P. Formulation and evaluation of meloxicam oral disintegrating tablet with dissolution enhanced by combination of cyclodextrin and ion exchange resins. *Drug Dev. Ind. Pharm.* **2015**, *41*, 1006−1016.
(53) Dua, K.; Pabreja, K.; Ramana, M. V. *Preparation, characterization and in vitro evaluation of aceclofenac solid dispersions*, 2010.
(54) Gupta, A. K.; Parasar, D.; Sagar, A.; Choudhary, V.; Chopra, B. S.; Garg, R.; Khatri, N. Analgesic and anti-inflammatory properties of gelsolin in acetic acid induced writhing, tail immersion and carrageenan induced paw edema in mice. *PLoS One* **2015**, *10*, No. e0135558.
(55) Viana, A. F.; Maciel, I. S.; Motta, E. M.; Leal, P. C.; Pianowski, L.; Campos, M. M.; Calixto, J. B. Antinociceptive activity of Trichilia catigua hydroalcoholic extract: new evidence on its dopaminergic effects. *Evid. Based Complement. Alternat. Med.* **2011**, *2011*, 120820 DOI: 10.1093/ecam/nep144.
(56) Woranam, K.; Senawong, G.; Utaiwat, S.; Yunchalard, S.; Sattayasai, J.; Senawong, T. Anti-inflammatory activity of the dietary supplement Houttuynia cordata fermentation product in RAW264. 7 cells and Wistar rats. *PloS one* **2020**, *15*, No. e0230645.
(57) Gupta, J.; Mohan, G.; Prabakaran, L.; Gupta, R. ACF loaded ethyl cellulose microspheres: Formulation designing, characterization and in-vivo antiinflammatory and analgesic activities in albino wistar rats. *Int. J. Drug Dev. Res.* **2014**, *6*, 133−144.
(58) Dinda, A.; Das, D.; Ghosh, G.; Kumar, S. Analgesic and anti-inflammatory activity of hydro-alcoholic extract of Azadirachta indica leaf. *Pharmacologyonline* **2011**, *3*, 477−484.
(59) Pillai, N. R.; Santhakumari, G. Anti-arthritic and anti-inflammatory actions of nimbidin. *Planta Med.* **1981**, *43*, 59−63.

https://doi.org/10.1021/acsomega.3c07065
ACS Omega 2023, 8, 48145−48158